Mechanochemical activation of class-B G-protein coupled receptor upon peptide-ligand binding

Cristina Lo Giudice[1], Haonan Zhang[2], Beili Wu[2], David Alsteens[1,]*

[1]Louvain Institute of Biomolecular Science and Technology, Université catholique de Louvain, Louvain-la-Neuve, Belgium.

[2]CAS Key Laboratory of Receptor Research, Shanghai Institute of Materia Medica, Chinese Academy of Sciences, Shanghai, China.

KEYWORDS. Atomic force microscopy, single-molecule force spectroscopy, human glucagon receptor, G-protein coupled receptors, mechanotransduction.

ABSTRACT

Glucagon binding to the class B G-protein-coupled glucagon receptor (GCGR) triggers the release of glucose from the liver during fasting. Recently, GCGR crystal structures have highlighted the conformation and molecular details of inactive and active receptor states. However, the dynamics of the conformational changes accompanying GCGR activation remains unclear. Here, we use multiplex force-distance curve-based atomic force microscopy (FD-based AFM) to probe *in situ* glucagon-binding to individual GCGRs and monitor dynamically the transition to the active conformer. After a "dock" step, in which glucagon is partially bound to the GCGR extracellular domain, further interactions of the N-terminus with the transmembrane domain trigger an increase in the stiffness of the complex adopting a highly stable and rigid "lock" conformer. This mechanotransduction is key for G-protein recruitment.

INTRODUCTION

G-protein-coupled receptors (GPCR), all sharing a common seven-transmembrane topology, represent the largest superfamily of transmembrane signaling proteins in humans[1]. Class B GPCR bind to their endogenous secretin-peptide ligands with both the ECD and TMD and are heavily implicated in hormone homeostasis and a variety of diseases[2]. Elucidating the kinetics and thermodynamics of ligand binding to G-protein-coupled receptors (GPCR), as well as the dynamics of the induced GPCR conformational changes is of key importance to understand their structure-function relationship and may aid for the design of effective drugs[1, 3].

Among secretin-like class B-GPCRs, due to its primary role in glucose homeostasis, GCGR represents one of the main therapeutic targets for type 2 diabetes and other diseases and metabolic syndromes, such as obesity, anxiety and depression[1,4]. Recently, the 3.0 Å-resolution crystallographic structure of the glucagon analogue NNC1702, in complex with GCGR has provided a deep understanding of the overall conformation and molecular interactions of the receptor in its activated state[5]. Scintillation proximity and cell-ligand binding assays showed that NNC1702 binding to GCGR results in a high affinity and stable conformer[5]. Structurally, NNC1702 forms an α-helical peptide spanning from the extracellular domain (ECD) to the transmembrane domain (TMD), establishing numerous interactions with GCGR. Among these interactions, the C-terminal part of the ligand interacts with the receptor ECD, the N-terminal part interacts mainly with the receptor TMD while the middle region of glucagon analogue forms key interactions with the GCGR stalk and ECL1 (Figure 1A). Interestingly, an important change of the relative orientation of the ECD and TMD is observed when comparing the inactive and active structures[6]. Differences also appear in the secondary structure of ECL1 and stalk from an extended β-sheet structure in the inactive ligand-GCGR complex to α-helices in the GCGR-NNC1702 complex. Overall, these conformational changes in the extracellular

region mirror further changes in the position of the transmembrane helices, particularly of helix VI that has a role in accommodating the Ras-like domain of the stimulatory G protein Gs[5, 7].

Unfortunately, little is known about the dynamics of the steps accompanying the receptor conformational changes towards its activation, which strongly limits our understanding of the class B receptors signal transduction mechanism. High-resolution structures of GPCRs and their complexes have proven to be difficult targets, often necessitating extensive engineering for the receptor stabilization into a particular state resulting in a loss of the dynamic aspects of the ligand-receptor complex formation and activation[2]. Current knowledge of GPCR activation relies mainly on ensemble studies or on molecular dynamics simulations[8] while direct evidence at the single molecule level is lacking. In this study, we use state-of-the-art FD-based AFM[9-12] to study dynamically the binding of glucagon and other peptide hormones to human GCGR and to decipher the impact on conformational changes, obtaining first direct insights into class B GPCRs activation.

RESULTS

GCGR protruding height determined by AFM

Human GCGRs were reconstituted in DOPC/cholesterol hemisuccinate liposomes to preserve their natural environment, adsorbed on mica and imaged at the single receptor level by FD-based AFM (Figure 1B-C and Figure S1). Topographical images show interconnected patches of supported lipid bilayer with randomly distributed GCGRs recognized as small, sparse protrusions. We analysed the height of the apo-GCGR and NNC1702-GCGR complex by imaging the same sample area before and after incubation with the peptide ligand (Figure 1D-G). Upon NNC1702 ligand injection, we observed that some receptors showed an increased height in the order of 5-20 Å, while no topographical change was detected for other receptors (Figure 1G). The height distribution analysis revealed a broader distribution and a shift toward

higher height values upon incubation with NNC1702 compared to apo-GCGRs (Figure 1H, I). The broader distribution can be deconvoluted as the sum of two receptor populations, centred at 2.5 nm and 3.6 nm and accounting for ≈ 56% and ≈ 44% of the receptors, respectively. Strikingly, the mean height value of the second population matches with the extracellular height of the receptor in its active conformation[5, 7], therefore representing the NNC1702-GCGR complexes having undergone a change in the receptor conformation. The fact that approximately 50% of receptors exhibit this behavior result from the GCGR reconstitution step into proteoliposomes, a step during which receptors lose their preferential orientation[13]. In absence of ligand the receptor orientation cannot be resolved, due to the size similarity of extracellular and cytosolic GCGR domains and to the high flexibility of the ECD domain that can be easily compressed and shifted during the AFM scanning. Conversely, in presence of NNC1702, correctly oriented GCGR can interact with the peptide, leading to the formation of the active GCGR-NNC1702 conformer, thus allowing us to discriminate between receptors exposing the extracellular domain and receptors exposing the cytosolic tail. To further evidence this loss of preferential orientation, we performed FD-based AFM with tips specifically functionalized to target either the cytoplasmic side or the extracellular side (Figure S2). Then, we designed a S2A/E9A/R18A-NNC1702 analogue peptide (AAA-peptide) (Figure S3) to drastically impair the interactions of the middle region and the N-terminal region with the ECL1, ECL2 and TMD regions of the receptor, while preserving the interactions of the C-terminal part of the peptide with the ECD of the GCGR[5]. Interestingly, after AAA-peptide injection, no marked change in the height distribution is observed (Figure 1J). Our analysis revealed the possibility to discriminate topographically not only between the apo- and ligand-bound GCGR, but also between different stages of peptide-GCGR complex formation. Notably, the interactions with the N-terminal and middle part of the peptide appear to play a crucial role in the receptor conformational change to the active state.

Peptide free-energy landscape to GCGR

We next used AFM tips functionalized with NNC1702 or substitute peptides to probe ligand-binding forces to GCGR at the single-molecule level as a function of the loading rate (LR, *i.e.* the speed at which the force is applied) and to reconstruct ligand-binding energy landscapes by FD-based AFM (Figure 2). The peptide-functionalized tip (Figure 2A) was cyclically approached and retracted from the GCGR substrate either in a sinusoidal (peak-force tapping mode) or rectangular (force-volume mode) manner. The combination of multiple FD-based modes allows us to cover a wide range of LRs. While with peak-force tapping we reach high-spatial resolution and acquire events in the high LR range, in the far-from-equilibrium regime, force-volume gives us the flexibility of variating independently the retraction speed, greatly extending the range of accessible LRs in the near-to-equilibrium regime[14]. FD curves with specific adhesive peaks (showing an extension profile compatible with the extension of the PEG linker before ligand rupture) were extracted selectively from the receptors areas and analysed (Figure S4). Upliftingly, we observed a significantly ($p=0.0081$) broader force distribution for the NNC1702 compared to the AAA-peptide (Figure 2B and Figure S5A-B). To discern the relative contribution of the middle and N-terminal region of the peptide to the broadening of the distribution, two other NNC1702 analogue peptides were designed to gradually restore the abolished interactions, S2A/E9A/R18D-NNC1702 analogue peptide (AAD-peptide) and S2A/E9A-NNC1702 analogue peptide (AAR-peptide)(Figure S3). Interestingly, while a gradual increase in the force distribution broadness was observed upon restoration of the interactions in the middle part, the initial broadness of the NNC1702-GCGR distribution is never reached (Figure 2B), indicating a pivotal contribution of the N-terminal part of the peptide, particularly in the high force range (Figure 2C-F). These results led us to the hypothesis that the broader force distribution corresponds to two different binding states of the NNC1702-GCGR complex, one at lower forces (binding state 1) and one at a higher force range (binding

state 2). This is confirmed by the analysis of the force distribution for the NNC1702-GCGR complex (Figure S5C) revealing a two-peak Gaussian distribution for the different LR ranges while for the AAA-peptide the second population remains negligible. For the two other peptide substitutes, we observed an intermediate situation, in which the population of rupture events at higher forces intensifies with the restoration of the interactions in the middle part. Force-LR dependencies were fitted with the Friddle-Noy-De Yoreo model[14-16] (Figure 2C-F) to get a quantitative estimation of the thermodynamic and kinetic parameters describing the ligand-binding free-energy landscape (Table S1).

Strikingly, we found that NNC1702 binding state 1 possesses very similar thermodynamic and kinetic values to AAR-peptide, while NNC1702 binding state 2 shows a much higher kinetic stability and a much lower dissociation constant, comparable to glucagon binding properties observed in bulk measurements[5, 17-18]. This observation underlines the key contribution of the positively charged residue R18 in the peptide middle region for the first binding step toward binding state 1, as also confirmed by the two other mutants that are thermodynamically less favoured. According to these results, binding state 1 and 2 represent two sequential conformers, in which the late binding of the NNC1702 N-terminus leads to a full, highly stable NNC1702-GCGR state.

Ligand-induced conformational and mechanical changes

To provide evidence for a possible conformational change upon ligand-binding to GCGR *in situ*, we further exploited the multiplexing profile of FD-based AFM by extracting the receptor height while probing GCGR with functionalized tip (Figure 3A-B). Similar to what we observed during NNC1702 injection experiments (Figure 1I), the GCGR height distribution measured with the NNC1702-functionalized tips is broader and can be deconvoluted into two populations that we previously attributed to apo-/inactive- and activated-GCGR states, respectively. The

145 percentage of the second population progressively decreases upon larger mutations in the
146 NNC1702 sequence (NNC1702>AAR-peptide>AAD-peptide>AAA-peptide) and matches
147 with the peptide binding properties (Figure 2C-F and table S1). In light of the binding properties
148 obtained above, we note that the conformational transition, i.e. the reorientation of the ECD, is
149 initiated during the binding of the ligand to the first state, suggesting a step-by-step mechanism.
150 Moreover, NNC1702 ligand binding correlates directly with the topography of interacting
151 GCGRs (Figure S6), which possess a significantly higher height compared to not interacting
152 receptors (i.e. GCGRs not correctly oriented/not available for binding, see Figure S2), further
153 supporting our hypothesis of agonist-peptide induced GCGR conformational transition.
154 Then, we investigated further the kinetics of the conformational rearrangements of the ECD
155 relative to the TMD leading to receptor activation. As the full binding of glucagon, like other
156 peptide hormones in class B GPCRs, forms a rigid helical structure spanning from the ECD to
157 the TMD, we hypothesized that the multiple interactions in the final binding state would result
158 in a restriction of the orientation freedom between the ECD and TMD and would therefore be
159 accompanied by a modification of the mechanical properties of the ligand-GCGR complex[19].
160 Thus, we tried to follow conformational change dynamics based on receptor stiffness properties.
161 To this end, we increased the surface delay using the force-volume mode providing more time
162 for the ligand-GCGR interaction and conformational transition; and we monitored the
163 mechanical properties (stiffness) of the NNC1702-GCGR complex by extracting the effective
164 spring constant k_{eff} (Figure 3C-D). Strikingly, we observed for NNC1702 two k_{eff} populations,
165 crossing around 12 $pN \cdot nm^{-1}$, suggesting the co-existence of two complexes with different
166 mechanical properties (Figure 3D and Figure S7). In addition, the frequency of the second
167 population (> 12 $pN \cdot nm^{-1}$) follows a first order association kinetics (Figure 3E). The rate
168 constant of the conformational switch (k_{conf}) indicates a time constant required for receptor
169 activation τ_{conf} of ~58 ms, which is much slower than the class A rhodopsin receptor[20-21] but in

good agreement with values obtained by FRET for class C GPCRs that also contain large extracellular binding domains[22]. This conformational change was not observed for the AAD-peptide (Figure 3E and Figure S7), confirming that complete binding of the N-terminal part of ligand is a prerequisite to reach the final activated state. Excitingly, this change in conformation is associated with an overall stiffening, probably resulting from the contraction of the distance between the ECD and the TMD. This strong mechanical coupling could facilitate structural rearrangements in the TMD, leading to crosstalk with the intracellular G proteins.

Glucagon triggers mechanotransduction

Structural studies (X-ray, cryo-EM) still require strategies to stabilize receptors into stable conformations, often using antibodies, nanobodies, ligand analogues or allosteric ligands in addition or in place of native biological ligands[23-25]. Being a dynamic technique, FD-based AFM does not suffer these limitations, therefore we were able to investigate GCGR binding to its endogenous ligand glucagon in native conditions (Figure 4). The experiments confirmed that glucagon binding to GCGR produces a similar conformational change as observed for NNC1702. Indeed, we also observed an increase in the receptor height with an activated population accounting for ≈ 45% of the total receptors, in good agreement with what observed for NNC1702 (Figure 4A). Next, glucagon and NNC1702 GCGR-binding characteristics are very similar, *i.e.* two binding states that possess very similar thermodynamic and kinetic properties (Figure 4B and Table S1), although the lifetime of the glucagon binding state 2 is lower. The higher lability of binding state 2 can be explained with D9E substitution of NNC1702, which introduced to stabilize the crystal structure of the complex[5], impedes the further movement of helix VII[26]. Finally, glucagon binding to GCGR also induced a time-dependent receptor stiffening with a τ_{conf} of ~46 ms, very similar to what we observed for NNC1702 binding, highlighting a common GCGR activation mechanism for agonist peptide

hormones (Figure 4C). Interestingly, we tracked in a dynamic manner the conformational steps using the kernel density estimation of the rupture force as a function of the complex stiffness upon agonist peptides binding (Figure 4D). A main population appears for low contact time (~10 ms) having binding ruptures and stiffness associated to the binding state 1. Upon time, a gradual increase in complex stiffness is observed (25 ms) indicating a dynamical change in the complex conformation, which is then followed by an increase in rupture forces (400 ms) when the final conformation is reached. These stiffness changes associated with the glucagon binding to the lowest affinity state emphasize that ligand binding to the ECD acts as a biomechanical switch in a purely biochemical transduction pathway. Interestingly, the force increase is accompanied by a slight decrease in the rigidity of the peptide-GCGR complex, possibly connected to the rearrangement of the GCGR TMD to expose the protein-Gα binding pocket.

DISCUSSION

The driving force underlying large-scale rearrangements upon ligand binding remains one of the most intriguing questions in GPCR activation and in particular for class B GPCRs for which drastic changes in the relative orientation of the ECD are observed[27]. Recent crystal[5] and cryo-EM[7] structures of the activated complex evidenced these structural rearrangements while failing to provide a detailed picture of the activation dynamics. Most GPCRs exhibit a basal range of dynamic conformations spanning from inactive to active states[1, 28]. Agonist ligands shift this equilibrium toward the activated states triggering large conformational changes. For the GCGR, glucagon binding is most probably responsible for the conformational change of the ECD relative to the TMD leading to receptor activation[18]. Our biophysical study revealed a « dock and lock » ligand-binding mechanism (Figure 4E). After an initial, high-affinity recruitment of the C-terminal glucagon end by the ECD («dock»), the captured peptide engages the TMD region through interaction of R18 within the middle part of the glucagon peptide. The

interactions of the middle part of the peptide cover a key role in triggering a GCGR rearrangement that facilitates the insertion of the glucagon N-terminus within the TMD and its subsequent interactions with the binding pocket («lock»). This conformational change is accompanied by a gradual ($\tau \sim 50$ ms) but marked increase in the rigidity of the structure. This stiffening, possibly resulting from the restriction of orientation freedom of the ECD and TMD and the contraction of the distance in the glucagon binding pocket, is likely to favour consecutive rearrangements within the TMD GCGR region to accommodate the G-protein complex, further shifting the equilibrium towards GCGR-induced intracellular signalling. This indicates a mechanotransduction mechanism of class B GPCR signal propagation, in which the initial biochemical input provided by glucagon triggers a mechanical change in GCGR that finally results in the G-protein recruitment and initiates the signalling cascade.

In conclusion, multiplex FD-based AFM enabled us to dynamically collect the topographical and binding parameters underlying the transition of GCGR from its inactive to its active conformation directly *in situ* and at the single-receptor level. To our knowledge, this is the first report exploiting the combination of high-resolution topography and single-molecule force spectroscopy to resolve the transition between two ligand-receptor binding states. Our results shed new light on the mechanisms of the glucagon-induced GCGR activation with an unprecedented level of temporal resolution and structural correlation, greatly expanding our knowledge of class B GPCR signal transduction, based on the sophisticated interplay between biochemical and mechanical signals.

ASSOCIATED CONTENT

Supporting Information. Detailed methods. Supplementary Figures 1-5, Supplementary Table 1. (PDF)

AUTHOR INFORMATION

Corresponding Author

*david.alsteens@uclouvain.be

Author Contributions

The manuscript was written through contributions of all authors. All authors have given approval to the final version of the manuscript.

Funding Sources

This work was supported by the Université catholique de Louvain and the Fonds National de la Recherche Scientifique (F.R.S.-FNRS; grant numbers: PDR T.0090.15 to D. Alsteens), the European Molecular Biology Organization (EMBO) (ALTF 542-2018 to CL). D.A. is a Research Associate at the FNRS.

Notes

The authors declare no competing financial interest.

ABBREVIATIONS

GCGR, human glucagon receptor; GPCR, G-protein-coupled receptor; FD-based AFM, force-distance curve-based atomic force microscopy; ECD, extracellular domain; TMD, transmembrane domain; ECL1, extracellular loop 1.

REFERENCES

1. Katritch, V.; Cherezov, V.; Stevens, R. C., Structure-function of the G protein-coupled receptor superfamily. *Annual review of pharmacology and toxicology* **2013,** *53*, 531-56.
2. Hollenstein, K.; de Graaf, C.; Bortolato, A.; Wang, M. W.; Marshall, F. H.; Stevens, R. C., Insights into the structure of class B GPCRs. *Trends in pharmacological sciences* **2014,** *35* (1), 12-22.
3. Rosenbaum, D. M.; Rasmussen, S. G. F.; Kobilka, B. K., The structure and function of G-protein-coupled receptors. *Nature* **2009,** *459* (7245), 356-363.
4. Cho, Y. M.; Merchant, C. E.; Kieffer, T. J., Targeting the glucagon receptor family for diabetes and obesity therapy. *Pharmacology & therapeutics* **2012,** *135* (3), 247-78.
5. Zhang, H.; Qiao, A.; Yang, L.; Van Eps, N.; Frederiksen, K. S.; Yang, D.; Dai, A.; Cai, X.; Zhang, H.; Yi, C.; Cao, C.; He, L.; Yang, H.; Lau, J.; Ernst, O. P.; Hanson, M. A.; Stevens, R. C.; Wang, M. W.; Reedtz-Runge, S.; Jiang, H.; Zhao, Q.; Wu, B., Structure of the glucagon receptor in complex with a glucagon analogue. *Nature* **2018,** *553* (7686), 106-110.
6. Zhang, H.; Qiao, A.; Yang, D.; Yang, L.; Dai, A.; de Graaf, C.; Reedtz-Runge, S.; Dharmarajan, V.; Zhang, H.; Han, G. W.; Grant, T. D.; Sierra, R. G.; Weierstall, U.; Nelson, G.; Liu, W.; Wu, Y.; Ma, L.; Cai, X.; Lin, G.; Wu, X.; Geng, Z.; Dong, Y.; Song, G.; Griffin, P. R.; Lau, J.; Cherezov, V.; Yang, H.; Hanson, M. A.; Stevens, R. C.; Zhao, Q.; Jiang, H.; Wang, M. W.; Wu, B., Structure of the full-length glucagon class B G-protein-coupled receptor. *Nature* **2017,** *546* (7657), 259-264.
7. Zhang, Y.; Sun, B.; Feng, D.; Hu, H.; Chu, M.; Qu, Q.; Tarrasch, J. T.; Li, S.; Sun Kobilka, T.; Kobilka, B. K.; Skiniotis, G., Cryo-EM structure of the activated GLP-1 receptor in complex with a G protein. *Nature* **2017,** *546* (7657), 248-253.
8. Latorraca, N. R.; Venkatakrishnan, A. J.; Dror, R. O., GPCR Dynamics: Structures in Motion. *Chemical reviews* **2017,** *117* (1), 139-155.
9. Alsteens, D.; Gaub, H. E.; Newton, R.; Pfreundschuh, M.; Gerber, C.; Müller, D. J., Atomic force microscopy-based characterization and design of biointerfaces. *Nature Reviews Materials* **2017,** *2* (5), 17008.
10. Lo Giudice, C.; Dumitru, A. C.; Alsteens, D., Probing ligand-receptor bonds in physiologically relevant conditions using AFM. *Analytical and Bioanalytical Chemistry* **2019,** *411* (25), 6549-6559.
11. Casuso, I.; Rico, F.; Scheuring, S., Biological AFM: where we come from – where we are – where we may go. *Journal of Molecular Recognition* **2011,** *24* (3), 406-413.
12. Leung, C.; Hodel, A. W.; Brennan, A. J.; Lukoyanova, N.; Tran, S.; House, C. M.; Kondos, S. C.; Whisstock, J. C.; Dunstone, M. A.; Trapani, J. A.; Voskoboinik, I.; Saibil, H. R.; Hoogenboom, B. W., Real-time visualization of perforin nanopore assembly. *Nature Nanotechnology* **2017,** *12* (5), 467-473.
13. Pfreundschuh, M.; Alsteens, D.; Wieneke, R.; Zhang, C.; Coughlin, S. R.; Tampé, R.; Kobilka, B. K.; Müller, D. J. Identifying and Quantifying Two Ligand-Binding Sites While Imaging Native Human Membrane Receptors by AFM. *Nat. Commun.* **2015**, 6 (1), 8857.
14. Friddle, R. W.; Noy, A.; De Yoreo, J. J., Interpreting the widespread nonlinear force spectra of intermolecular bonds. *Proceedings of the National Academy of Sciences* **2012,** *109* (34), 13573.
15. Alsteens, D.; Pfreundschuh, M.; Zhang, C.; Spoerri, P. M.; Coughlin, S. R.; Kobilka, B. K.; Muller, D. J., Imaging G protein-coupled receptors while quantifying their ligand-binding free-energy landscape. *Nature methods* **2015,** *12* (9), 845-851.
16. Mulvihill, E.; Pfreundschuh, M.; Thoma, J.; Ritzmann, N.; Müller, D. J., High-Resolution Imaging of Maltoporin LamB while Quantifying the Free-Energy Landscape and Asymmetry of Sugar Binding. *Nano Letters* **2019,** *19* (9), 6442-6453.
17. Authier, F.; Desbuquois, B., Glucagon receptors. *Cellular and Molecular Life Sciences* **2008,** *65* (12), 1880-1899.

18. Shimizu, I.; Hirota, M.; Ohboshi, C.; Shima, K., Identification and localization of glucagon-like peptide-1 and its receptor in rat brain. *Endocrinology* **1987,** *121* (3), 1076-82.
19. Yang, L.; Yang, D.; de Graaf, C.; Moeller, A.; West, G. M.; Dharmarajan, V.; Wang, C.; Siu, F. Y.; Song, G.; Reedtz-Runge, S.; Pascal, B. D.; Wu, B.; Potter, C. S.; Zhou, H.; Griffin, P. R.; Carragher, B.; Yang, H.; Wang, M.-W.; Stevens, R. C.; Jiang, H., Conformational states of the full-length glucagon receptor. *Nature Communications* **2015,** *6* (1), 7859.
20. Lohse, M. J.; Nuber, S.; Hoffmann, C., Fluorescence/bioluminescence resonance energy transfer techniques to study G-protein-coupled receptor activation and signaling. *Pharmacological reviews* **2012,** *64* (2), 299-336.
21. Leach, K.; Gregory, K. J., Molecular insights into allosteric modulation of Class C G protein-coupled receptors. *Pharmacological research* **2017,** *116*, 105-118.
22. Grushevskyi, E. O.; Kukaj, T.; Schmauder, R.; Bock, A.; Zabel, U.; Schwabe, T.; Benndorf, K.; Lohse, M. J., Stepwise activation of a class C GPCR begins with millisecond dimer rearrangement. *Proceedings of the National Academy of Sciences of the United States of America* **2019,** *116* (20), 10150-10155.
23. Surade, S.; Blundell, Tom L., Structural Biology and Drug Discovery of Difficult Targets: The Limits of Ligandability. *Chemistry & Biology* **2012,** *19* (1), 42-50.
24. Rasmussen, S. G. F.; Choi, H.-J.; Fung, J. J.; Pardon, E.; Casarosa, P.; Chae, P. S.; DeVree, B. T.; Rosenbaum, D. M.; Thian, F. S.; Kobilka, T. S.; Schnapp, A.; Konetzki, I.; Sunahara, R. K.; Gellman, S. H.; Pautsch, A.; Steyaert, J.; Weis, W. I.; Kobilka, B. K., Structure of a nanobody-stabilized active state of the β2 adrenoceptor. *Nature* **2011,** *469* (7329), 175-180.
25. Deupi, X.; Edwards, P.; Singhal, A.; Nickle, B.; Oprian, D.; Schertler, G.; Standfuss, J., Stabilized G protein binding site in the structure of constitutively active metarhodopsin-II. *Proceedings of the National Academy of Sciences of the United States of America* **2012,** *109* (1), 119-24.
26. Unson, C. G.; Andreu, D.; Gurzenda, E. M.; Merrifield, R. B., Synthetic peptide antagonists of glucagon. *Proceedings of the National Academy of Sciences of the United States of America* **1987,** *84* (12), 4083-7.
27. Parthier, C.; Reedtz-Runge, S.; Rudolph, R.; Stubbs, M. T., Passing the baton in class B GPCRs: peptide hormone activation via helix induction? *Trends in biochemical sciences* **2009,** *34* (6), 303-10.
28. Kobilka, B. K.; Deupi, X., Conformational complexity of G-protein-coupled receptors. *Trends in pharmacological sciences* **2007,** *28* (8), 397-406.

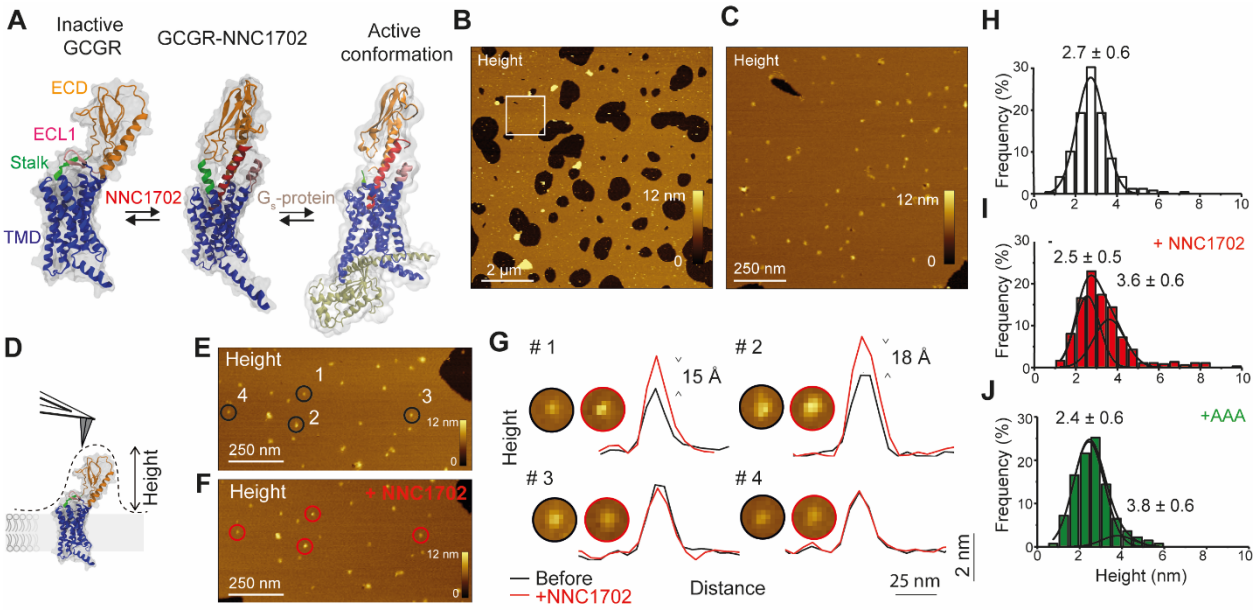

345

346 **Figure 1.** Structure and AFM topography of Apo-GCGR and GCGR complexes with peptide
347 ligands. (A) Crystal structures of inactive GCGR-NNC0640-mAb1 complex (left, PDB ID
348 5XEZ, antibody not shown) and of active GCGR-NNC1702 complex (centre, PDB ID 5YQZ).
349 For comparison, the cryo-EM structure the active GLP-1—GLP-1R—Gs complex is reported
350 (right, PDB ID 5VAI, Gβ and Gγ not shown). The receptor ECD, stalk, ECL1 and TMD, the
351 peptide ligands and the G-proteins are coloured orange, green, magenta, blue, red, and light
352 green, respectively. (B) AFM height image of Apo-GCGRs embedded in a DOPC/cholesterol
353 hemisuccinate lipid bilayer (peak-force tapping mode, oscillation frequency 2 kHz, amplitude
354 50 nm). (C) Zoomed image from B (white square). (D) The height of the domains protruding
355 from the lipid bilayer is extracted. (E) Overview of Apo-GCGRs topography (peak-force
356 tapping mode, oscillation frequency 2 kHz, amplitude 50 nm). (F) Overview of GCGRs
357 topography after 30 min incubation with NNC1702 (peak-force tapping mode, oscillation
358 frequency 2 kHz, amplitude 50 nm). (G) Zoomed topographs and cross-sections from four
359 GCGR receptors extracted from E (black circles/lines) and F (red circles/lines). Receptors 1-2
360 show an increase in height upon NNC1702 incubation, while for receptors 3-4 no change in
361 height was observed. (H-J) Height distributions of Apo-GCGR (n = 248) (H), GCGR-NNC1702
362 complex (n = 235) (I) and GCGR-AAA peptide complex (n = 139) (J).

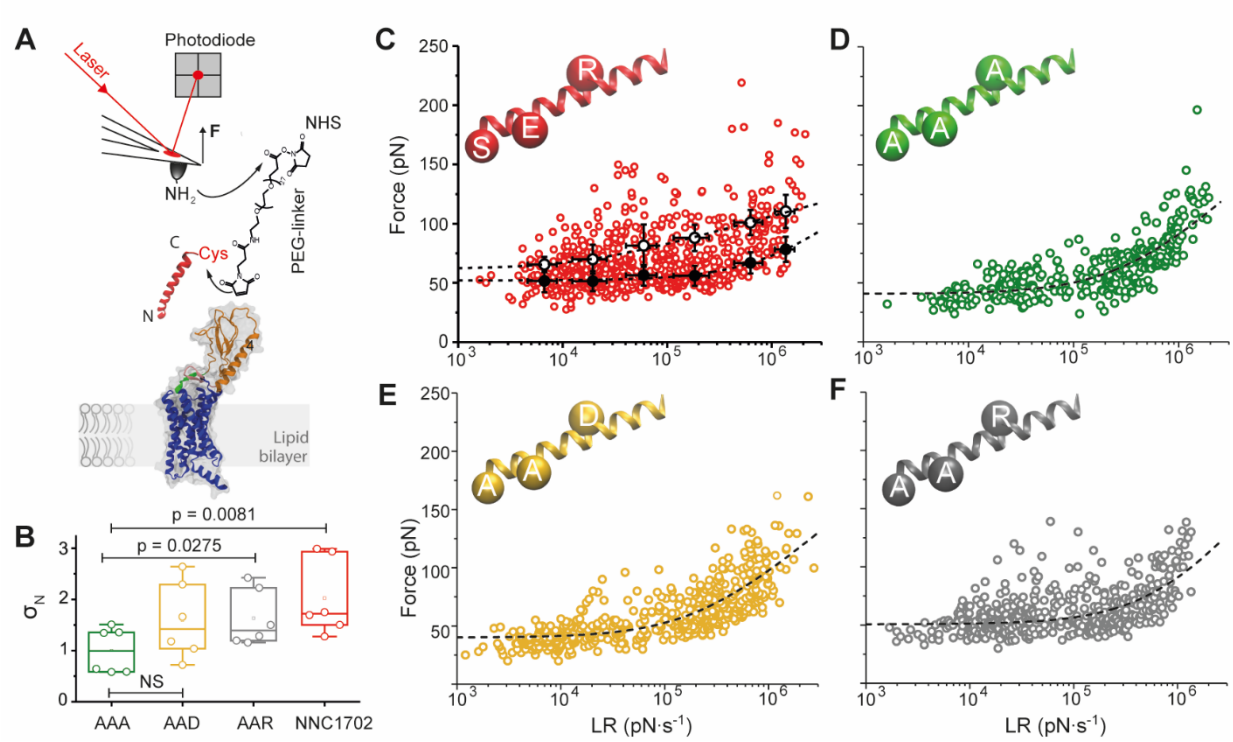

Figure 2. FD-based AFM of single-peptide ligand receptor bonds reveals multiple GCGR-ligand binding states. (A) Peptide ligands were covalently immobilized on AFM tips through a C-terminal cysteine. (B) Dispersion of force data cloud for GCGR-ligand complexes. For each peptide ligand, the unbinding forces have been divided into six ranges, according to the LR and fitted with a monomodal Gaussian distribution. The mean of the standard deviation values (σ) of the distributions obtained for each LR range is taken as indication of the dispersion of the force data cloud for each peptide ligand (standard deviation values σN are normalized by the mean of AAA-peptide, P-values determined by one-tailed unpaired t-test). (C-F) Dynamic force spectroscopy (DFS) plots for GCGR interactions with NNC1702 (n = 703) (C), AAA-peptide (n = 341) (D), AAD-peptide (n = 520) (E) and AAR-peptide (n = 462) (F). The data reflect the combination of force-volume mode (at retraction speeds 2 μm·s^{-1} and 6 μm·s^{-1}) and peak-force tapping mode (oscillation frequency 0.25 kHz, amplitude 50 nm) (see methods and Figure S4). The corresponding Friddle-Noy-De Yoreo fit is overlapped (black dashed lines). For NNC1702 (C), the average unbinding forces per LR range for binding state 1 (full dots) and binding state 2 (empty black dots) have been determined by multi-Gaussian fit of the force histogram for each LR and used for the Friddle-Noy-De Yoreo fit (dashed black lines).

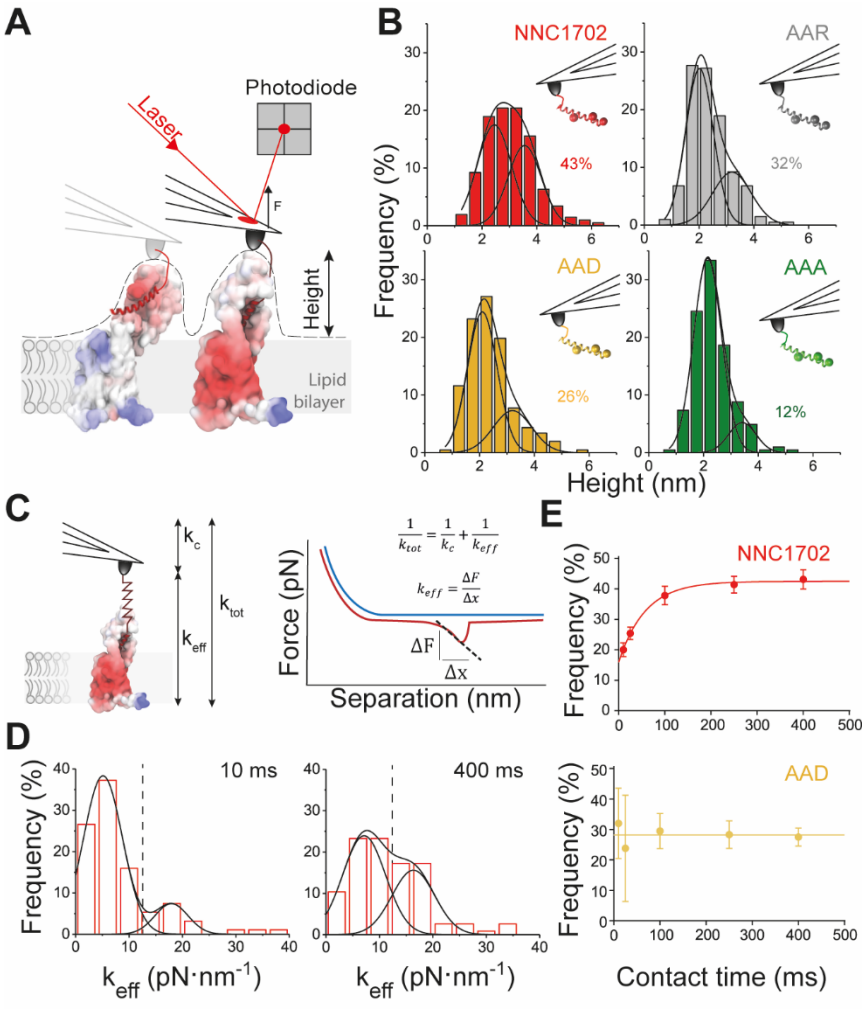

380

381 **Figure 3.** *In situ* dynamic mapping of NNC1702-GCGR binding and transition to the activated
382 state. (A) Peptide-functionalized AFM tips are used to induce GCGR transition to the receptor
383 active state at the single-receptor level. The receptor conformational change is quantified by
384 measuring its height with respect to the lipid bilayer. (B) Height distributions of GCGR in
385 complex with NNC1702 (red, n = 206), AAR-peptide (grey, n = 206), AAD-peptide (yellow, n
386 = 207) and AAA-peptide (green, n = 204). The GCGR height values were extracted from high-
387 resolution peak-force tapping images (oscillation frequency 0.25 kHz, amplitude 50 nm). (C)
388 The spring constant (k_{tot}) is the combination of the cantilever stiffness (k_c) and the stiffness of
389 the PEG-ligand-GCGR complex (k_{eff}). Force-volume experiments (retraction speed 2 μm·s^{-1})
390 were performed introducing increasing surface delays. k_{tot} was extracted from the force-distance
391 curves as the slope just before bond rupture and used to infer k_{eff}. (D) k_{eff} distributions at 10 ms
392 (left, n = 96) and 400 ms (right, n = 116) NNC1702-GCGR contact time. In both, a bimodal k_{eff}
393 distribution is found, with the two populations crossing between the third and fourth data bin
394 (k_{eff} 12 pN·nm^{-1}). (E) Frequency of k_{eff} values > 12 pN·nm^{-1} as a function of ligand-receptor

contact time for NNC1702 (red) and NNC1702-S2 (yellow). Error bars have been calculated to account for uncertainty in the overlapping area between the two populations.

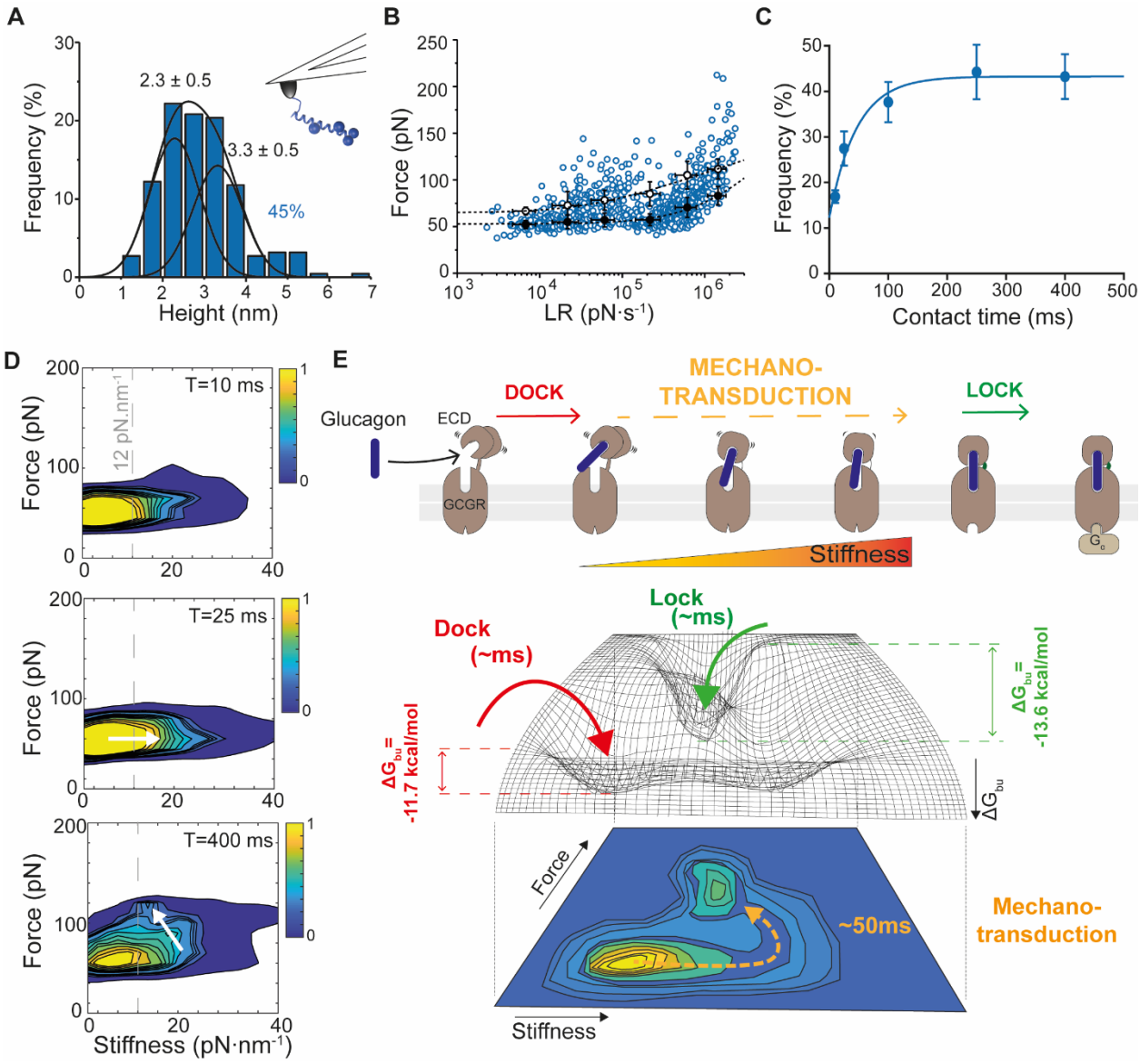

397

398 **Figure 4.** Glucagon-GCGR binding mechanism and *in situ* ligand–induced receptor activation.
399 (A) Height distribution of glucagon-GCGR complexes acquired *in situ* with glucagon-
400 functionalized tips (n = 221) (peak-force tapping mode, oscillation frequency 0.25 kHz,
401 amplitude 50 nm). (B) Force *vs* loading rate plots for glucagon-GCGR interactions (n = 832).
402 The data reflect the combination of force-volume mode (at retraction speeds 2 μm·s^{-1} and 6
403 μm·s^{-1}) and peak-force tapping mode (oscillation frequency 0.25 kHz, amplitude 50 nm). The
404 Friddle-Noy-De Yoreo fit (dashed lines) is used to reconstruct the ligand-receptor binding free
405 energy lansdcape for binding state 1 (full dots) and 2 (empty dots). (C) Frequency of k_{eff} values
406 > 12 pN·nm^{-1} as a function of glucagon-GCGR contact time. (D) Force *vs* stiffness density plots
407 of NNC1702-GCGR and glucagon-GCGR complexes at 10 ms (top, n = 165), 25 ms (middle,

n = 205), and 400 ms (bottom, n = 190) contact time. (E) Proposed mechanism of glucagon-induced GCGR activation.

410 ToC graphic

411